

DETERMINATION OF α_s
FROM A DIFFERENTIAL JET MULTIPLICITY
DISTRIBUTION AT SLC AND PEP¹

SACHIO KOMAMIYA

Representing the Mark II Collaboration

*Stanford Linear Accelerator Center, Stanford University,
Stanford, California 94309*

ABSTRACT

We measure the differential jet multiplicity distribution in e^+e^- annihilation with the Mark II detector. This distribution is compared with the second order QCD prediction and α_s is determined to be $0.123 \pm 0.009 \pm 0.005$ at $\sqrt{s} \approx M_Z$ (at SLC) and $0.149 \pm 0.002 \pm 0.007$ at $\sqrt{s} = 29$ GeV (at PEP). The running of α_s between these two center of mass energies is consistent with the QCD prediction. The Q^2 dependence of the $\Lambda_{\overline{MS}}$ determination is also discussed.

1. INTRODUCTION

In determining $\Lambda_{\overline{MS}}$ (or α_s), it is better to use observables which are insensitive to fragmentation and higher order QCD effects. In that respect, the commonly used observables are (1) the total hadronic cross section (σ_{tot}), (2) the energy-energy-correlation asymmetry (EECA) and (3) the three-jet-event fraction. However, σ_{tot} is not easy to measure precisely enough to determine $\Lambda_{\overline{MS}}$ because the QCD effect is small (approximately 5% of σ_{tot}). The EECA is expected to be relatively insensitive to effects associated with fragmentation. However, it turns out that the effects are not so small³ and hence extensive studies of these effects are needed to estimate the corresponding systematic errors.³ The three-jet event fraction appears relatively insensitive to fragmentation effects, if one chooses a reasonable jet algorithm and if one deals only with hard three-jet events.⁴ However, the actual dependence of the three-jet event fraction on the jet resolution parameter (y_{cut}) used to select hard three-jet events is not statistically easy to handle. This problem can be solved by using a differential jet multiplicity as described below.

* This work was supported in part by Department of Energy contract DE-AC03-76SF00515 (SLAC).

¹ This report is presented at the 15th APS Division of Particles and Fields General Meeting, Houston, Texas, January 3-6, 1990 and is based on the paper by the Mark II Collaboration.¹ The experimental method using a differential jet multiplicity was presented at the International Europhysics Conference (EPS meeting) in Madrid, September 1989.²

2. DIFFERENTIAL JET MULTIPLICITY

To define the number of jets (jet multiplicity) in an event we use the algorithm proposed by the JADE collaboration.⁵ The scaled invariant mass cut-off (y_{cut}) is used for the jet resolution in the algorithm. The algorithm proceeds as follows:

For each particle (cluster) pair i, j , the scaled invariant mass

$$y_{ij} = \frac{2E_i E_j (1 - \cos \chi_{ij})}{E_{vis}^2}$$

is calculated, where E_i and E_j are the energy of the particles (clusters) and χ_{ij} is the angle between them. The particle (or cluster) pair with the smallest y_{ij} is combined by adding the 4-momenta of the two particles (clusters) i and j to form a new cluster $i + j$ ($p_{i+j}^\mu = p_i^\mu + p_j^\mu$). The above clustering procedure is repeated until all the clusters satisfy the condition $y_{ij} > y_{cut}$ where y_{cut} is referred to as the jet resolution. The three-jet fraction $f_3(y_{cut})$ is defined to be the number of three-jet events obtained with the algorithm, divided by the total number of hadronic events. The two-jet fraction $f_2(y_{cut})$ and the four jet fraction $f_4(y_{cut})$ are similarly defined.

This jet algorithm has the important feature that mapping from parton jets to hadron jets in Monte Carlo hadronic events is close to one-to-one for reasonably large y_{cut} (≥ 0.04) values.⁴ However, it is not easy to extract α_s by fitting the $f_3(y_{cut})$ (or $f_2(y_{cut})$) distribution because the same events contribute at different y_{cut} values and one must take into account all the correlations in this distribution.

To overcome this difficulty, a differential jet multiplicity is defined in the following way. The clustering is terminated when the number of jets has reached a pre-selected value n , irrespective of y_{ij} values. For each event, particles are assigned to n -jets using this method and y_n is defined to be the minimum value of the scaled invariant mass $y_{ij} = M_{ij}^2/E_{vis}^2$ ($i \neq j$, $i, j = 1, 2, \dots, n$). In other words, y_n is the y_{cut} value corresponding to the transition from n -jet to $(n-1)$ -jet for a given event. The distribution function of y_n is denoted $g_n(y_n)$. Integrating $g_3(y_3)$ over y_3 from 0 to y_{cut} , one recovers $f_2(y_{cut})$ because all the events with $y_3 < y_{cut}$ are categorized as two-jet events for the given resolution y_{cut} .

Hence,
$$g_3(y_3)|_{y_3=y_{cut}} = \frac{\partial}{\partial y_{cut}} f_2(y_{cut}).$$

Similarly,
$$g_4(y_4)|_{y_4=y_{cut}} = \frac{\partial}{\partial y_{cut}} [f_2(y_{cut}) + f_3(y_{cut})].$$

Note that only the leading term ($\propto \alpha_s^2$) is available for g_4 in second order QCD calculations. Similarly, $g_5(y_5)|_{y_5=y_{cut}} \equiv 0$ in second order. Therefore we restrict our analysis to the differential jet fraction $g_3(y_3)$ to determine α_s .

3. EXPERIMENTAL METHODS

Multihadron events are selected by requiring that the number of charged tracks is at least seven at SLC [at least five at PEP] and that the sum of charged and neutral particle energies (E_{vis}) is greater than $0.50\sqrt{s}$ at SLC [$0.55\sqrt{s}$ at PEP].⁴ The detection efficiency for multihadron events is estimated using QCD-based Monte Carlo generators⁸⁻¹⁰ to be 0.80 ± 0.02 at SLC [0.51 ± 0.02 at PEP]. A total of 391 events from the SLC data and 7348 events from the PEP data pass the selection cuts.

Second order perturbative QCD predictions are directly compared with the measured g_3 distribution for determining α_s . Detector effects, biases due to event selection and initial state radiation effects are corrected with bin-by-bin correction factors. In the range $0.04 \leq y_3 \leq 0.14$, the corrections are typically less than 5% for SLC data [10% for PEP data]. The bin-to-bin systematic errors due to the variation of the correction factors for various models⁸⁻¹⁰ are less than 4% at SLC [3% at PEP]. These errors slightly increase with y_3 . The overall normalization uncertainty in the correction factors is estimated to be 2% at SLC [3% at PEP]. The corrected $g_3^{\text{corr}}(y_3)$ distributions for the two data samples are shown in Fig.1.

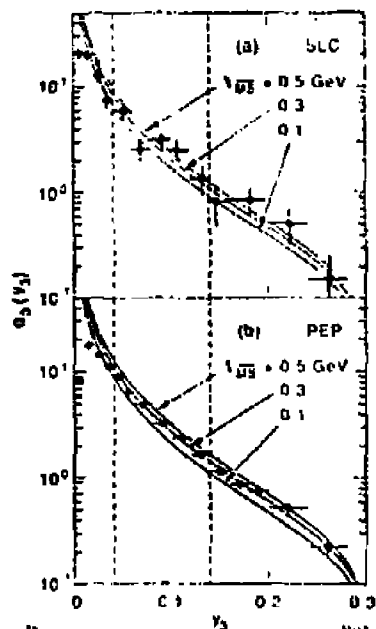


Fig.1:
 The experimental distributions of y_3 at (a) $\sqrt{s} = 91$ GeV, and (b) $\sqrt{s} = 20$ GeV. Only the statistical errors are indicated in the figures. The curves below $y_3 = 0.14$ indicate the QCD predictions with $\Lambda_{\overline{\text{MS}}\bar{\text{F}}} = 0.1$ GeV, 0.3 GeV and 0.5 GeV for $Q^2 = s$. The y_3 range used in the fit for the determination of α_s is defined by the two dashed lines. The curves above $y_3 = 0.14$ are extrapolated from the QCD predictions in the low y_3 range.

⁴ In order to reduce the bias due to initial state radiation and background from two photon processes for the PEP data, events with large missing energy or with a large energy photon are eliminated by applying additional cuts described in Ref.6. For the Z -resonance data such effects are small, hence we do not apply any cuts other than those mentioned above.⁷

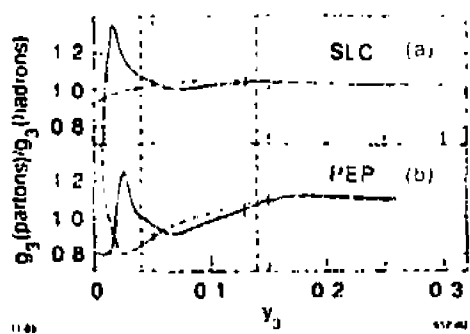


Fig 2:

The ratio $g_3^{\text{partons}}/g_3^{\text{hadrons}}$ as a function of y_3 for partons and for hadrons (after fragmentation and decay of unstable particles) at (a) $\sqrt{s} = 91$ GeV, and (b) $\sqrt{s} = 29$ GeV. The solid curve corresponds to the Lund model based on $\mathcal{O}(\alpha_s^2)$ matrix element and the dashed curve to the Lund parton shower model. The error bars indicate the Monte Carlo statistical errors.

Corrections are not applied for fragmentation effects. Rather, they are accounted for as systematic errors. In Fig.2, the ratio $g_3^{\text{partons}}/g_3^{\text{hadrons}}$ is shown as a function of y_3 for two models.^{8,10} In the range $0.04 \leq y_3 \leq 0.14$, the bin-to-bin systematic errors associated with fragmentation effects are 3-5% at SLC [5-10% at PEP]. The normalization uncertainty is estimated to be 2% at SLC [4% at PEP].

4. RESULTS (RUNNING α_s)

The α_s value is obtained from a fit of the corrected $g_3(y_3)$ distribution to the $\mathcal{O}(\alpha_s^2)$ QCD prediction.¹¹ The fit is performed within the range of $0.04 \leq y_3 \leq 0.14$ using a likelihood method which accounts for the statistical errors and the various systematic errors. The lower y_3 limit of the fitted range is chosen in order to limit the fragmentation effects, while the upper limit arises only because the QCD prediction for $y_3 > 0.14$ is not available in Ref.11. Choosing the renormalization point Q^2 to be s , we obtain

$$\begin{aligned}\alpha_s &= 0.123 \pm 0.009 \pm 0.005 & \text{at SLC,} \\ \alpha_s &= 0.149 \pm 0.002 \pm 0.007 & \text{at PEP.}\end{aligned}$$

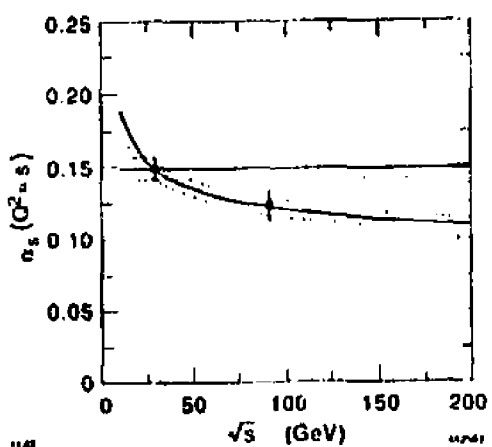


Fig.3:

The strong coupling $\alpha_s(Q^2 = s)$ as a function of \sqrt{s} . The errors include statistical and systematic uncertainties added in quadrature. Also shown are the extrapolations of the α_s measurement at $\sqrt{s} = 29$ GeV to higher energies using the formula of Ref.12, or assuming a constant α_s . The dotted lines indicate the extrapolation of the measured $\alpha_s \pm 1\sigma$ from 29 GeV.

The running of α_s from 29 GeV to 91 GeV is consistent with the QCD predic-

tion, as shown in Fig.3. The running of α_s with Q^2 is governed by the Renormalization Group Equation (RGE) which, to second order in α_s , is given by

$$\frac{\partial}{\partial \ln Q^2} \frac{\alpha_s}{2\pi} = -b_0 \left(\frac{\alpha_s}{2\pi} \right)^2 \left(1 + b_1 \frac{\alpha_s}{2\pi} \right) .$$

The coefficients b_0 and b_1 do not depend on the renormalization scheme chosen, hence they represent fundamental physical quantities. Denoting by n_f the effective number of flavors at a given Q^2 , QCD predicts $b_0 = (33 - 2n_f)/6$ and $b_1 = (153 - 19n_f)/(33 - 2n_f)$. The RGE can be integrated to express b_0 in terms of our two measurements of the coupling constant α_s^{SLC} and α_s^{PEP} and of the $\ln Q^2$ variation $\Delta \ln Q^2 = 2 \ln (91/29) = 2.29$. One gets

$$b_0 = \frac{F(\alpha_s^{SLC}) - F(\alpha_s^{PEP})}{\Delta \ln Q^2}, \quad \text{with} \quad F(\alpha_s) = \frac{2\pi}{\alpha_s} - b_1 \ln \left(\frac{2\pi}{\alpha_s} + b_1 \right) .$$

We obtain $b_0 = 3.4^{+2.1}_{-1.4}$ where the errors take into account the partial cancellation of the normalization uncertainties. This value, which is almost independent of b_1 , agrees with the QCD prediction of $b_0 = 3.83$ for $n_f = 5$.

To express the α_s measurements in terms of the QCD scale parameter $\Lambda_{\overline{MS}}$, we use the approximate solution of the RGE given in Ref.12. We obtain $\Lambda_{\overline{MS}} = 0.29^{+0.17+0.11}_{-0.12-0.06}$ GeV at SLC, and $\Lambda_{\overline{MS}} = 0.28^{+0.02+0.08}_{-0.02-0.07}$ GeV at PEP, in agreement with the value $0.33 \pm 0.04 \pm 0.07$ GeV previously obtained using the energy-energy-correlation by Mark II at 29 GeV.³

5. Q^2 DEPENDENCE OF $\Lambda_{\overline{MS}}$

In finite order perturbative QCD, the predictions depend on the renormalization scheme (RS) and on the renormalization point (Q^2). Therefore the Λ_{QCD} value, which is extracted from the data using finite order QCD predictions, depends on both the RS and the Q^2 . Triggered by the work of Kramer and Lampe,¹³ several experimental papers were published in an attempt to optimize Q^2 for the determination of $\Lambda_{\overline{MS}}$.¹⁴⁻¹⁷ The simultaneous determination of Q^2 and $\Lambda_{\overline{MS}}$ using jet multiplicity favors very small Q^2 values,^{16,17} but the results are very sensitive to perturbative QCD predictions in the very soft region where the size of the second order term is large compared to the first order term (i.e. where the $\mathcal{O}(\alpha_s^2)$ perturbative expansion is not reliable). Therefore the results of simultaneous determination of Q^2 and $\Lambda_{\overline{MS}}$ would be based on the instability of the $\mathcal{O}(\alpha_s^2)$ perturbative expansion in the infrared region, and hence is highly questionable. If we restrict ourselves only in the region where we expect the fragmentation and higher order QCD effects to be small, $\Lambda_{\overline{MS}}$ and Q^2 cannot be determined independently. For example, using $g_1(y_{cut})$ in the range $0.04 \leq y_3 \leq 0.14$, where $\mathcal{O}(\alpha_s^2)$ perturbative QCD works well, the resultant one sigma contour in the $\Lambda_{\overline{MS}}-Q^2$ plane is a band

along a curve starting from $\Lambda_{\overline{MS}} = 0.1$ GeV at $Q^2 = (3 \text{ GeV})^2$ and extending to $\Lambda_{\overline{MS}} = 2.3$ GeV at $Q^2 = (1000 \text{ GeV})^2$.

In the second order calculations, difference of the predictions for different RS 's can be absorbed into the ' Q^2 ambiguity'.¹⁸ Therefore ' RS ambiguity' and ' Q^2 ambiguity' are degenerated, to the $\mathcal{O}(\alpha_s^2)$. A reasonable renormalization point Q^2 must be chosen as we choose the \overline{MS} scheme for RS .*

Several prescriptions have been proposed to choose a particular value of Q^2 .¹⁹⁻²¹ For the purpose of illustrating and exploring the effect of the choice of Q^2 , we use the Brodsky-Lepage-Mackenzie (BLM) method²¹ to eliminate the Q^2 ambiguity for g_3 at each y_3 value. In this picture, the source of the running α_s is the vacuum polarization of gluons (in analogy with QED), hence Q^2 might be the typical momentum scale involved in the vacuum polarization loops; the energy scale is related to the allowable invariant mass (virtuality) of gluons, which can be as small as a few GeV. The choice of Q^2 depends on the kinematical variable y_3 because the gluon virtuality depends on y_3 . The Q value prescribed by the BLM method (Q^*) is 4 GeV [1.3 GeV] at $y_3 = 0.05$ and increases to 6 GeV [2.0 GeV] at $y_3 = 0.10$ for $\sqrt{s} = 91$ GeV [$\sqrt{s} = 29$ GeV]. Choosing $Q^2 = (Q^*)^2$ at each value of y_3 and \sqrt{s} , and n_f values appropriate to the small Q^* values ($n_f = 4$ for SLC and $n_f = 3$ for PEP), the $\Lambda_{\overline{MS}}$ values obtained using the BLM method are $0.17^{+0.08+0.05}_{-0.06-0.03}$ GeV at SLC and $0.17^{+0.01+0.03}_{-0.01-0.03}$ GeV at PEP. These $\Lambda_{\overline{MS}}$ values are smaller than the values which are determined with $Q^2 = s$.

6. CONCLUSIONS

We have presented the measurement of the coupling strength of the strong interaction in e^+e^- annihilation at $\sqrt{s} \approx M_Z$ (SLC) and at $\sqrt{s} = 29$ GeV (PEP) using the differential jet multiplicity g_3 . The method is relatively insensitive to fragmentation effects and statistically easy to handle. In the framework of second order QCD calculations and for $Q^2 = s$, the measured values of α_s are $0.123 \pm 0.009 \pm 0.005$ at $\sqrt{s} = 91$ GeV and $0.119 \pm 0.002 \pm 0.007$ at $\sqrt{s} = 29$ GeV. The running of α_s from 29 GeV to 91 GeV is seen and is consistent with the QCD prediction. The corresponding values of the QCD scale parameter are $\Lambda_{\overline{MS}} = 0.29^{+0.17+0.11}_{-0.12-0.06}$ GeV at SLC, and $\Lambda_{\overline{MS}} = 0.28^{+0.02+0.08}_{-0.02-0.07}$ GeV at PEP. For comparison, results have been also presented at considerably smaller values of the renormalization point (Q^2), as suggested, for example, by the Brodsky-Lepage-Mackenzie method.

* Conventionally, $Q^2 = s = q_{\gamma^*, g}^2$ is chosen for e^+e^- collision and $Q^2 = -q_{\gamma^*}^2$ for deep inelastic lepton-nucleon scattering. However, these choices are not directly connected to the $q\bar{q}g$ vertex where α_s should be determined.

REFERENCES

1. Mark II Collab., S. Komamiya and F. Le Diberder et al., Phys. Rev. Lett. **64**, 987 (1990).
2. S. Komamiya, SLAC-PUB-5154, to be published in the Proceedings of Int. Europhysics Conf. on High Energy Physics, Madrid Spain, September 1989.
3. Mark II Collab., D.R. Wood et al., Phys. Rev. D**37**, 3091 (1988).
4. JADE Collab., S. Bethke et al., Phys. Lett. B**213**, 235 (1988); Mark II Collab., S. Bethke et al., Z. Physik C**43**, 325 (1989).
5. JADE Collab., W. Bartel et al., Z. Physik, C**33**, 23 (1986).
6. Mark II Collab., A. Petersen et al., Phys. Rev. D**37**, 1 (1988).
7. Mark II Collab., G.S. Abrams et al., Phys. Rev. Lett. **63**, 1558 (1989).
8. The Lund parton shower model, T. Sjöstrand, Comp. Phys. Comm. **39**, 347 (1986); T. Sjöstrand and M. Bengtsson, Comp. Phys. Comm. **43**, 367 (1987).
9. The Webber parton shower model, G. Marchesini and B.R. Webber, Nucl. Phys. B**238**, 1 (1984); B. R. Webber, Nucl. Phys. B**238**, 492 (1984).
10. The Lund model based on $\mathcal{O}(\alpha_s^2)$ matrix elements calculated by T.D. Gottschalk and M. P. Shatz, Phys. Lett. B**150**, 451 (1985).
11. G. Kramer and B. Lampe, Fortschr. Phys. **37**, 161 (1989).
12. Particle Data Group, M. Aguilar-Benitez et al., Phys. Lett. B**170**, 78 (1986).
13. G. Kramer and B. Lampe, Z. Physik, C**39**, 101 (1988).
14. N. Magnussen, PhD thesis, Universität Wuppertal, 1988.
15. CELLO Collab., H.J. Behrend et al., Z.Phys. C**44**, 63 (1989).
16. S. Bethke, Z. Physik, C**43**, 331 (1989); AMY Collab., I.H. Park et al., KEK-89-53, submitted to the Lepton Photon Symposium (Stanford, 1989).
17. OPAL Collab., M.Z. Akrawy et al., Phys. Lett. B**235**, 389 (1990).
18. for example, K. Hagiwara, Suppl. Progr. of Theor. Phys. **77**, 100 (1983).
19. G. Grunberg, Phys. Lett. B**95**, 70 (1980).
20. P.M. Stevenson, Phys. Rev. D**23**, 2916 (1981).
21. S. Brodsky, G.P. Lepage and P.B. Mackenzie, Phys. Rev. D**28**, 226 (1983).